A fibre Bragg grating sensor system monitors operational load in a wind turbine rotor blade

2006 Meas. Sci. Technol. 17 1167

(http://iopscience.iop.org/0957-0233/17/5/S39)

INSTITUTE OF PHYSICS PUBLISHING MEASUREMENT SCIENCE AND TECHNOLOGY

Meas. Sci. Technol. **17** (2006) 1167–1172 doi:10.1088/0957-0233/17/5/S39

A fibre Bragg grating sensor system monitors operational load in a wind turbine rotor blade

Kerstin Schroeder[1], Wolfgang Ecke[1], Jörg Apitz[2], Elfrun Lembke[2] and Gerhard Lenschow[3]

[1] Institute for Physical High-Technology (IPHT), Albert-Einstein-Str. 9, D-07745 Jena, Germany
[2] Jenoptik LOS GmbH, Göschwitzer Straße 25, D-07745 Jena, Germany
[3] Enercon GmbH, Dreekamp 5, D-26605 Aurich, Germany

E-mail: kerstin.schroeder@ipht-jena.de

Received 19 July 2005, in final form 6 February 2006
Published 13 April 2006
Online at stacks.iop.org/MST/17/1167

Abstract
A fibre Bragg grating sensor system has been installed and successfully operated in a horizontal-axis wind turbine since February 2004. We herewith report the requirements, design and construction parameters of the sensor system for continuous on-line monitoring of bending loads of the rotor blades and provide examples of the monitoring results.

Keywords: fibre-optic sensor, strain monitoring, wind turbine blade monitoring, fibre Bragg grating sensor system, health monitoring, continuous-operation alternating-load monitoring

1. Introduction

The size and power of modern wind turbines have been continuously increasing during recent years. Key components and technologies of wind turbines experience tremendous changes in order to improve efficiency and lifetime at reduced material investment. Typically, these new systems will be installed in off-shore wind parks where maintenance and repair are important cost factors, but also increasingly in topographically structured terrain with frequently varying wind attitudes, which leads to higher peak loads at the wind turbines. In this context, load monitoring of wind turbines experiences increasing importance.

Load monitoring using strain sensors in the rotor blades has the advantage of providing additional information on the load history of the blades and, consequently, one can carry out lifetime estimations of the rotor blades [1].

Mainly because of their lightning safety and neutrality to electro-magnetic interference, fibre-optic (FO) strain sensors are advantageously applied in wind turbine structural monitoring [2]. Out of the broad range of FO strain sensors, fibre Bragg gratings (FBGs) have the advantage of a direct physical correlation between the measured Bragg wavelength and strain. Recalibration of the sensors is not necessary, even after the signal-processing unit has been exchanged. The wavelength-encoded sensor signal cannot be disturbed by influences on the transmission lines, and their multiplexing in extended sensor networks provides results of spatial load distributions along very few optical fibre lines [3, 4].

The requirements on the durability of a sensor system in wind turbines are very high: it should not be influenced by steady rotations, vibrations, mechanical shocks, electromagnetic fields and environmental temperature changes over an expected lifetime of >20 years. To get real-time strain profiles, exact simultaneity of sampling the strain state of all sensors must be ensured.

This paper describes an FBG measurement system designed to fulfil these requirements which is currently monitoring the 53 m long rotor blade of a 4.5 MW wind turbine (type E112, see figure 1) in a wind park at Wilhelmshaven, Germany.

2. The sensor system

The FGB sensor network is wavelength multiplexed, the Bragg wavelengths of the individual sensors in the network are measured utilizing broadband spectral illumination and spectrometric read-out of the sensor network reflection signals

Figure 1. 4.5 MW horizontal-axis wind turbine type E112, selected for operational load monitoring using fibre-optic sensor technology. Photograph: Enercon GmbH.

(scheme of signal-processing unit (SPU) in figure 2). The SPU has been developed as a robust and potentially low-cost instrument for operation in a heavy-loaded industrial or aerospace environment [5]. The main components of the SPU are as follows:

- superluminescent diode broadband light source (type SLD381, Superlum Diodes Ltd), fibre-pigtailed, optical output power <100 μW, operational spectral range $\lambda =$ 810–860 nm limited by the drop of spectral power density to 15% of maximum;
- compact polychromator, based on imaging diffractive grating (100 mm base length) and 2048-pixel CCD photo-receiver line covering the 720–890 nm wavelength range [6].

The polychromator, based on a spectral read-out principle, ensures the simultaneous processing of all sensor signals in the network and provides momentary states of vibrational strain modes. The duration of measurement intervals (integration time τ_i of the CCD photo-receiver line) amounts typically to $\tau_i = 1$ ms, the only source of time incoherence is the light travel time between the individual sensors in the network of $\delta\tau_i < 0.4$ μs. Bragg wavelengths are calculated as the result of a sub-pixel approximation (e.g., Gaussian correlation fit) to the intensities of ± 7 CCD pixels around every sensor peak maximum in the reflected spectrum, corresponding to a spectral width of ± 0.6 nm.

The sensitivity of the relative Bragg wavelength shift $\Delta\lambda_B/\lambda_B$ to the strain of the optical fibre (i.e., to its relative elongation $\Delta L/L$) depends on the fibre's effective photoelastic coefficient p as the only experimental calibration parameter:

$$\Delta L/L = \Delta\lambda_B/\lambda_B/(1-p).$$

The experimental value of p for the used fibre type, $p = 0.23$, has been measured once on a calibrated bending beam and was found to be constant within the operational strain, temperature and wavelength ranges, ± 5000 $\mu\varepsilon$, -40 to $+180$ °C and 800–860 nm, respectively.

Repeatability of Bragg wavelength measurement (1σ value) amounts to $\delta\lambda_B \sim 0.4$ pm, corresponding to a repeatability of strain measurements of 0.7 $\mu\varepsilon$. Corresponding to the spectral integration width of ± 0.6 nm, peak broadening by fast strain shifts is approximated as a time-averaged peak position for strain rates of up to 500 $\mu\varepsilon$ ms^{-1}, which cannot be exceeded in wind turbines.

The accuracy of absolute strain measurements depends mainly (apart from the sensor attachment, see below) on the long-term stability of the spectrometer. For a passive compensation of the effect of SPU temperature on wavelength read-out, this dependence has been experimentally measured, and it is numerically compensated using on-line SPU temperature measurement results. Then, maximum long-term reproducibility errors of Bragg wavelengths amount to 15 pm. For further improvement, a stabilized reference FBG has been incorporated in the SPU. Considering its wavelength read-out, absolute wavelength errors are decreased to <5 pm.

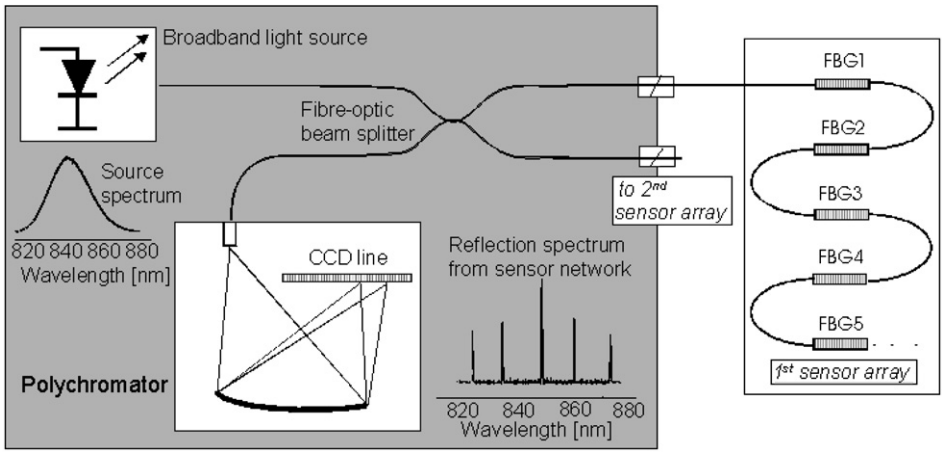

Figure 2. Diagram of the FBG sensor signal-processing unit.

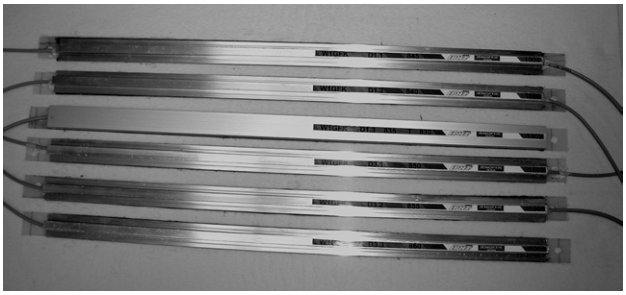

Figure 3. Photograph of the six sensor pads for strain monitoring in the rotor blade. The third pad includes a temperature sensor.

The FBG sensors have a spectral width of 0.1–0.3 nm and reflectivity of 30–90%. The reflectivity values of the individual FBG sensors are fitted to the source spectrum in order to achieve a nearly equally levelled peak spectrum in the polychromator. The FBG sensors have been inscribed (an excimer laser at 248 nm, Bragg grating adjustment by interference fringes of a Talbot interferometer) in a previously acrylate-coated single-mode optical fibre for 800 nm operation wavelength, which has been loaded with hydrogen at 200 bar for several days and annealed at 100 °C after the FBG inscription process.

The power supply (220 V/50 Hz) is available in the rotating nacelle. However, the data transmission from the SPU in the wind turbine rotor to the data handling computer in the stator is carried out via a class I Bluetooth wireless RS232 interface.

Fibre-optic signal transmission between SPU and sensor arrays is accomplished via fibre-optic connectors with high reflection loss (type E2000/HRL, Diamond SA). While these connectors are sufficiently vibration-proof (according to Bellcore standard), further shielding of the connectors and of the whole interior of the SPU against dust and humidity is accomplished using additional sealed lead-through of the fibre-optic cables (diameter 3 mm, Kevlar strain relief) between nacelle and SPU housing.

3. FBG sensor pads

FBGs as intrinsic fibre-optic strain sensors can be embedded directly into the glass fibre reinforced plastics (GFRP) of the rotor blade, without major disturbances of the laminate. However, in this test installation, the FBG strain sensors have been integrated after finishing the rotor blade. Therefore, a sensor pad has been developed consisting of a GFRP substrate, with the FBG strain sensors attached frictionally stable to it, and a cord grip, providing strain relief to the fibre-optic signal transmission cables at both ends of the pad (figure 3).

In order to achieve the transfer of a locally averaged strain load of the blade material to the relatively short FBG strain sensor, we chose a very long sensor pad length of 400 mm, in comparison to the FBG sensor length of 5 mm. All attachments between FBG sensors and blade use adhesives over the whole FBG length to the pad and over the whole pad area to the blade surface, respectively.

Consequently, we measured the average strain over the pad length of 400 mm, bridging possibly shorter local strain gradients in the GFRP. To shield the sensors on the pads from possible damage during blade inspection and maintenance, the pads were covered with a plastic cap fixed to the GFRP pad by a flexible adhesive. Three strain sensor pads each have been attached to both the windward and the leeward internal surfaces of the blade, on opposite symmetrical positions (see scheme in figure 4).

The two parallel sensor lines on opposite wind positions have been installed in order to obtain redundant push–pull strain values for the flap-wise blade bending line. Using all of them, we can check either the function of the measurement system itself or the anti-symmetry of the strain conditions on both the windward and leeward blade surfaces.

Then, the measurement results of two strain sensors D1 and D3 in an anti-symmetric position for flap-wise bending strain can be used for an effective compensation of temperature effects:

(a) actually applied flap-wise bending strain: $\varepsilon_{\mathrm{D1}} = -\varepsilon_{\mathrm{D3}}$;
(b) additional temperature effect on apparently measured strain values:

$$\varepsilon_{\mathrm{D1app}} = \varepsilon_{\mathrm{D1}} + (\Delta T \cdot C_T)_{\mathrm{D1}},$$
$$\varepsilon_{\mathrm{D3app}} = \varepsilon_{\mathrm{D3}} + (\Delta T \cdot C_T)_{\mathrm{D3}}.$$

The anti-symmetric bending strain ε can be obtained from $\varepsilon \approx (\varepsilon_{\mathrm{D3app}} - \varepsilon_{\mathrm{D1app}})/2$.

The measuring accuracy for obtaining absolute strain values is limited by possible differences of temperature T and temperature coefficients C_T of both strain sensors at their

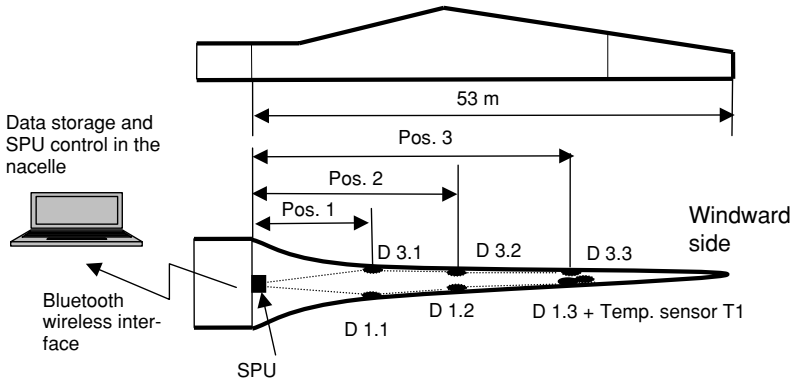

Figure 4. Scheme of the positions of sensor pads and signal-processing unit (SPU) in the rotor blade.

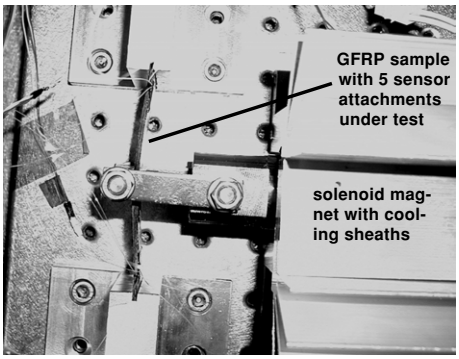

Figure 5. Photograph of the test set for application of periodic strain loads. Maximum strain cycle rate: 50 s^{-1}. Maximum strain amplitude: 2000 $\mu\varepsilon$.

different measuring sites. However, during a rotation cycle of the wind turbine (duration 5–10 s), the blade temperature can be assumed to be constant. The amplitudes of the bending load alternations during rotation cycles are most important for an estimation of structural degradation and are measured consequently with negligible temperature-induced errors.

For separate temperature measurements, we installed an additional FBG temperature sensor, mechanically decoupled at 1 mm distance from the blade surface, at position 3. Usually, it is possible to measure the temperature coefficient of the strain sensor and to use a temperature sensor nearby (i.e., an FBG sensor without mechanical contact) for numerical compensation of the influences of temperature changes. This compensation method works successfully for the case of small measuring objects, preferably of metals or other crystalline materials. However, the GFRP shows poor reproducibility and anisotropy of the coefficient α of thermal elongation; values of $\alpha = 18\text{–}25 \times 10^{-6}\,K^{-1}$ have been obtained during temperature calibration. Particularly in the extended blades, temperature changes in regions far distant from the sensor site cause general changes of the strain field. While this effect (as any other specific cause for the appearing strain) is not important for a sole material monitoring, it has to be considered for calculating a bending line.

As a qualitative estimation, a higher error of absolute strain results will be obtained from the separate measurement and compensation of temperature effects, as compared to the measurement of strain difference amplitudes in the push–pull strain sensor configuration. An experimental comparison in order to quantify the errors occurring in practice has still to be performed.

The strain transfer from the measuring object to the sensor element plays an important role in strain sensing and requires particular focus. Strain sensing is used very often for measurement of low and quasi-static strains. In such cases, very hard adhesives are necessary. For wind turbine blade monitoring, the strain sensors and their interfaces with the substrate have to withstand large strain changes, changing 10–15 times per minute, over more than 20 years of expected lifetime for the turbine. The strength of the attachment and its technology should be optimized for long lifetime under such specific load conditions.

To investigate the quality of different attachments, we used a strain load test arrangement driven by a solenoid magnet (figure 5). The stroke magnet can bend a GFRP beam with five test sensors attached to it at a rate of 50 load cycles per second to strain amplitudes of up to 2000 $\mu\varepsilon$. It can be adjusted to exert elongations as well as compressions and to bias a static load to the alternating strain loads.

Using this test arrangement, we checked the strain measurement results of sensors and their attachments over a 4-week period while exercising 1.3×10^8 load cycles. This compares to a wind turbine lifetime of 20 years at a rotation rate of 12 rpm (rpm: rotations per minute).

Three different types of sensor attachments have been under test. As compared to the most appropriate adhesive used in sample B, a hard adhesive in sample A tends to detach under compression, while a softer adhesive in sample C does not transfer the full strain amplitude as can be calculated from the bending beam characteristic. Sample B of these attachment types could withstand the full number of load cycles without degradation.

The diagrams in figure 6 show the strain measurement results of sensor sample B during strain cycles 87.5×10^6 to 137.5×10^6 (figure 6(*a*)) and a detailed section during

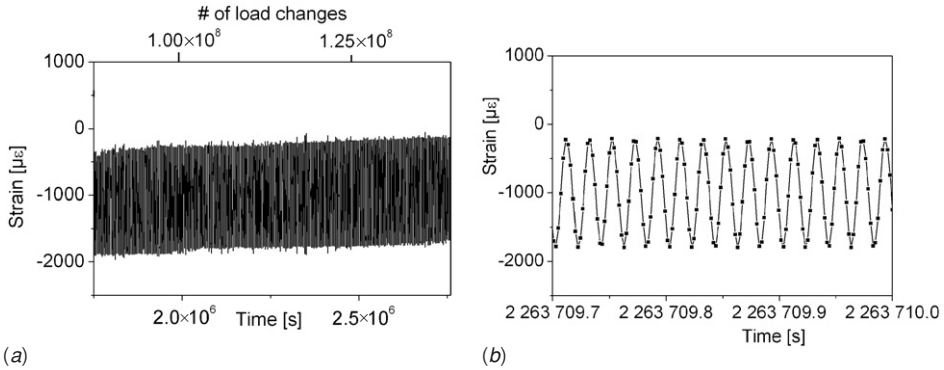

Figure 6. Measurement results of a continuously cycled strain load test: (*a*) finishing period of 500×10^6 cycles; (*b*) detailed section of 15 strain cycles. The strain amplitudes characterize the quality of the sensor attachment and are constant over the test period for this sensor type B. The slow offset drift is caused by a drift of the mechanical set-up (equally for all sensors during the test period).

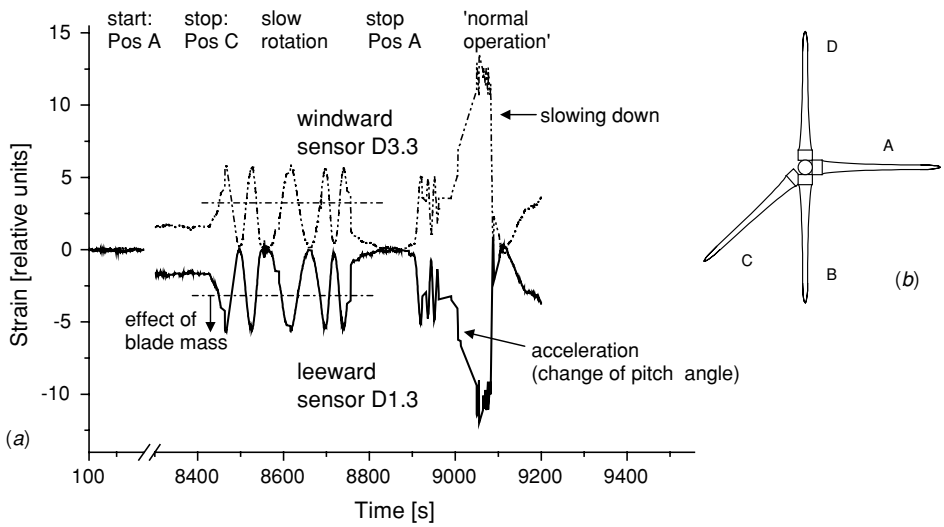

Figure 7. (*a*) Experimental results of sensor system characterization. (*b*) Definition of blade directions, Dir. A–Dir. D. Measured strain data in the diagram are provided for the FBG sensors D3.3 and D1.3, attached to opposite windward and leeward blade sides, at position 3 (definition of sensor positions in figure 4).

the cycles 113 335 490 to 113 335 505 (figure 6(*b*)). In figure 6(*a*), the band of the alternating sensor response is shown. The constant width of this band indicates the constant alternating strain amplitudes. In the detailed diagram of figure 6(*b*), the measurement regime is documented showing the load cycles at a rate of 50 s^{-1} and the strain measuring values obtained at a rate of 480 s^{-1}.

The fast load changes cause a temperature increase of the visco-elastic material because of internal friction [7], which was measured to be at a load cycle rate of 50 s^{-1} for sensor type sample B of about 5 K. For the GFRP composite material, the repeatability of thermal loads by visco-elasticity, and of the temperature coefficient of the Bragg wavelength as well, is rather poor, with variations of up to 15% under comparing measuring conditions. Nevertheless, the test results allow for a qualitative comparison of the sensor attachments. Of course, the slower rotation of the operational wind turbine will not cause any remarkable temperature increase in the adhesives.

4. Results

The sensor network was installed in October 2003, the first SPU ('StrainaTemp' [8] with three measurements per second) in February 2004. During and after installation of the SPU, the measurement system has been characterized, with an example of test results shown in figure 7.

Strain results are shown for an anti-symmetric sensor pair at mirrored windward and leeward positions, respectively. At the beginning of the measurement, the blade was positioned horizontally in direction Dir. A (see figure 7(*b*)). In this blade direction, the strain measurement system was set to zero (however, the actual zero strain would be obtained as the mean sensor strain value from measurements in Dir. B (upwards) and Dir. D (downwards), respectively, as shown by the dash-dot lines in figure 7(*a*)).

At the beginning of the diagram in figure 7(*a*), during seconds 8100 to 8430, the blade was turned to Dir. C and held in this position. In this period, the unfiltered 1σ noise level of the strain data is measured to be about 2 $\mu\varepsilon$. During seconds 8430 to 8770 in figure 7(*a*), the rotor moved at a slow rotation rate without substantial wind load, and the amplitudes of the measured strain corresponded to the deformation under the blade weight. The characteristic of the strain results shows the anti-symmetry between sensors D1.3 and D3.3.

After that, the rotor was moved back to Dir. A and, consequently, the strain values went back to the value defined as zero, too. Then, the blade pitch was changed in order to accelerate the rotation rate to the normal operation mode under wind load.

The measuring rate of this 'StrainaTemp' SPU type was too slow for a detailed study of strain transients, but it proved the practicability of the applied sensor technology during the first year of wind turbine operation without failure of sensors or SPU.

In November 2004, SPU 'StrainaTemp' was replaced by its faster successor 'StrainaTemp50' operating at a data rate of 50 measurements per second. 'StrainaTemp50' uses the same optical and opto-electronic set-up, but its digital signal processor performs the Bragg wavelength calculations already on-board [9] resulting in the faster transmission rate of the sensor data already calculated. These fast measurements provide more detailed strain data showing significant differences between the strain characteristics at different sensor positions along the blade. Figure 8 shows a data example taken during the normal operation of the E112.

The strain load of sensor D1.1 at a position near the rotor shaft (figure 8, curve 1, leeward position 1) has nearly sinusoidal characteristics, varying synchronously with the blade position during rotation. Contrary to curve 1, the strain response near the blade tip (sensor responses in curves 2 and 3 in figure 8) shows more structured characteristics, additionally consisting of higher as well as lower frequency components. The anti-symmetric responses from the opposed sensors D1.3 and D3.3 indicate this strain also as a localized flap-wise

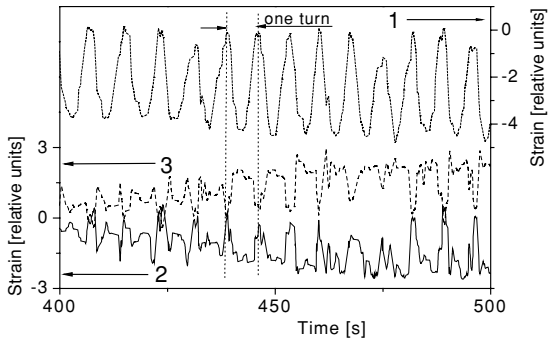

Figure 8. E112 operating at 8.4 rpm. Example of strain measurement results using 50 Hz FBG interrogation unit StrainaTemp50. (1) Sensor D1.1 on leeward blade side, near to rotor shaft at position 1. (2, 3) Sensor pair D1.3 and D3.3 on opposite leeward and windward blade sides, respectively, near to the tip of blade at position 3 (definition of sensor positions in figure 4).

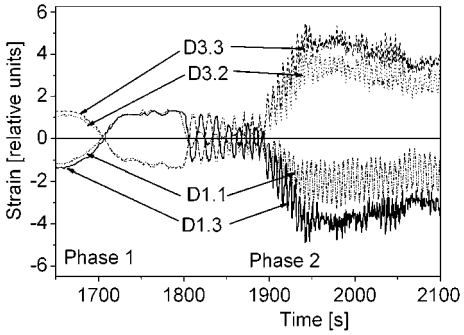

Figure 9. Results of load monitoring during acceleration of the turbine. Phase 1: slow rotation at 0.3 rpm; blades are loaded only by their own mass. Phase 2: acceleration to 11 rpm; blade bending under changing wind load (definition of sensor positions in figure 4).

bending behaviour, with superimposed wobbling near the free blade tips.

Figure 9 shows the load relations between strain sensors at different positions during an acceleration period of the wind turbine, with exact calibration of their zero strain values.

5. Conclusions

An FBG measurement system for load monitoring in horizontal-axis wind turbines has been installed and proved to work successfully. During more than 2 years of field test, the capability and reliability of the applied fibre-optic sensor technology have been assessed. The two sensor systems were ready to deliver continuous load monitoring results under the realistic environmental conditions in an operating wind turbine over their full test periods (about 1 year each at 4 measurements per second and at 50 measurements per second, respectively).

The on-line availability of blade strain data will be used for safety monitoring and active safety control of the blades and for load monitoring of the whole turbine. The accumulated strain data will be used for the determination of a fatigue load footprint as a diagnostic tool for the blade material and also for wind park site characterization. The detailed strain characteristics at different measurement sites along the blade are of interest for optimization purposes during further blade development.

Acknowledgments

The authors would like to express their sincere thanks to their colleagues at IPHT Jena, Ch Chojetzki for fibre Bragg grating inscription, M Kautz and Ch Mueller for preparation of the sensor pads and L Zoeller for opto-electronic implementations. The FBG signal-processing electronics has been developed and manufactured by Th Morgenstern and R Hultsch, Jeti GmbH Jena.

References

[1] Kensche C W and Söker H 2000 Lifetime prediction for GFRP fabrics comparing to WISPERX standard and a measured spectrum *DEWI Mag.* **16** 73–6

[2] Wernicke J, Shadden J, Kuhnt S, Byars R, Rhead P and Damaschke M 2004 Field experience of fibre optical strain sensors for providing real time load information from wind turbine blades during operation *Paper presented at the European Wind Energy Conf. 2004 (London, UK, 22–25 November)*

[3] Rao Y J 1997 In-fibre Bragg grating sensors *Meas. Sci. Technol.* **8** 355–75

[4] Othonos A and Kalli K 1999 *Fibre Bragg Gratings, Fundamentals and Application in Telecommunication and Sensing* (Boston, MA: Artech House)

[5] Ecke W, Latka I, Willsch R, Reutlinger A and Graue R 2001 Fibre optic sensor network for spacecraft health monitoring *Meas. Sci. Technol.* **12** 974–80

[6] Ecke W, Bartelt H, Schwotzer G, Usbeck K, Willsch R, Birkle S, Bosselmann T and Kraemmer P 1997 Low-cost optical temperature and strain sensing networks using in-line fiber gratings *Proc. SPIE* **3099** 390–7

[7] Dakin J P, Ecke W and Reuter M 2005 Comparison of vibration measurements of elastic and mechanically lossy (visco-elastic) materials, using fibre grating sensors *17th Int. Conf. on Optical Fibre Sensors, Proc. SPIE* **5855** 5–8 (Post-deadline papers)

[8] www.jenoptik.de

[9] Ecke W and Willsch R 2003 Field trial experience with fiber Bragg grating health monitoring systems and photochemical sensor concepts basing on polychromator signal processing *Proc. 16th Int. Conf. on Optical Fiber Sensors (IEICE, Japan)* pp 500–5